Computer Science and Interdisciplinary Research Journal
Volume 1, Issue 2, 2024, ISSN: 3033-1218, DOI: 10.70862/CSIR.2024.0102-07, 2024

Numerical Analysis of the Magnetic Moment in S/F/S-Josephson Junction

Elis Dieva

Paisii Hilendarski University of Plovdiv, 24 Tzar Asen, 4000 Plovdiv, Bulgaria

dievaelis@gmail.com

Abstract – One particularly intriguing object in superconductivity is the Josephson junction, which is an integral part of quantum computer hardware. Analysing this object requires solving differential equations. Such problems often cannot be solved with analytical methods; therefore, numerical methods and computational mathematics must be utilized. This article explores a fundamental model of the Josephson junction. The model presents the spatial coordinates of the magnetic moment as unknown functions dependent on time in a system of three ordinary differential equations with initial conditions. Comparative analysis of various methods is conducted for different sets of parameters. Optimal numerical methods for these particular instances of the problem are found. Visual results are also presented.

Keywords – numerical analysis, Josephson junction, magnetic moment.

1. Introduction

Modern science and technology are based on the modelling and analysis of complex systems representing physical, chemical, economic, and biological processes. These systems, which are defined by motion in space over time are often described by differential equations. In this context the Cauchy problem for systems of ordinary differential equations (ODEs) is one of the fundamental problems providing a framework for studying the dynamic behaviour of different systems [1]. Moreover, to present reliable results, they must meet conditions related to their accuracy. Implicit numerical methods known for their ability to handle stiff problems due to their stability and increased accuracy play an important role in numerical analysis.

Most commonly, a Josephson junction (Fig. 1) is composed of two superconductors separated by a thin layer of dielectric or ferromagnetic material [2]. It allows the passage of a superconducting current without voltage and energy loss.



Figure 1. Ferromagnetic Josephson junction (S/F/S)

When a current flows through a Josephson junction, it generates a magnetic field in the immediate vicinity of the junction [3]. The magnetic moment in the Josephson junction arises from the formation of currents known as Josephson currents which can create a magnetic field around the junction [4]. The magnetic moment is a physical quantity that describes the magnetic properties of particles, bodies, or systems. It is related to the distribution of magnetic charge or the movement of charged particles.

φ_0 and an S/F/S (superconductor/ferromagnet/ superconductor) Josephson junctions differ primarily in the mechanisms driving their behaviour [5, 6].

A φ_0-junction arises from broken inversion or time-reversal symmetry, typically due to spin-orbit coupling and an applied magnetic field, leading to a phase offset. In contrast, an S/F/S junction relies on the magnetic exchange field in the ferromagnetic layer, which induces oscillatory superconducting correlations and can stabilise ground states with phase differences of 0 or π. However, an S/F/S junction can exhibit φ_0-like behaviour when additional symmetry-breaking effects, such as noncollinear magnetization or spin-orbit coupling, are introduced. These effects

DOI: https://doi.org/10.70862/CSIR.2024.0102-07

Corresponding author: Elis Dieva,
University of Plovdiv Paisii Hilendarski
Email: dievaelis@gmail.com

Received: 4 December 2024.
Revised: 12 January 2025.
Accepted: 12 January 2025.
Published: 13 January 2025.

BY-NC-ND © 2024 Elis Dieva. This work is licensed under the Creative Commons Attribution-NonCommercial-NoDerivatives 4.0 International License.

The article is published with Open Access at http://csirjournal.com/

effectively merge the characteristics of both systems. This is the reason why in some cases the terms can be interchangeable.

In summary, the magnetic moment is an important concept in physics that describes how particles and systems interact with magnetic fields and how they create magnetic phenomena. The precession of the magnetic moment also plays an important role in the field of spintronics.

The magnetic moment in this S/F/S model of the Josephson junction can be described by a system of ordinary differential equations that requires initial conditions to be solved [7]. Through this Cauchy problem, the solutions that reflect the behaviour of the physical system are determined, taking into account external influences and parameters.

The primary mathematical model considers the phase difference of the Josephson junction as a linear function of time.

2. Problem Formulation

Let us assess the fundamental mathematical model of a Josephson junction, described by a system of three ODEs [7, 8].

$$\frac{dm_x}{dt} = \frac{\omega_F}{1+(M\alpha)^2}(-m_z m_y + Grm_z sin(\omega t - rm_y) - \alpha[m_x m_z^2 + Grm_x m_y sin(\omega t - rm_y)])$$

$$\frac{dm_y}{dt} = \frac{\omega_F}{1+(M\alpha)^2}(m_x m_z - \alpha[m_y m_z - Gr(m_z^2 + m_x^2) sin(\omega t - rm_y)])$$

$$\frac{dm_z}{dt} = \frac{\omega_F}{1+(M\alpha)^2}(-Grm_x sin(\omega t - rm_y) - \alpha[Grm_y m_z sin(\omega t - rm_y) - m_z(m_y^2 + m_x^2)])$$

where the initial conditions are
$m_x(0) = 0,\ m_y(0) = 0,\ m_z(0) = 1.$

The unknown functions here (m_x, m_y and m_z) are the spatial coordinates of the magnetic moment, represented as functions of time. As can be seen, the problem is multi-parameter with the following parameters:

- ω_F: resonance frequency of the ferromagnet;
- α: damping parameter;
- G: parameter of phase difference coupling;
- r: spin-orbit coupling parameter;
- ω: ratio of the phase difference to time;
- M: norm of the magnetic moment.

3. Numerical Approach

For the numerical solving of the system in this investigation, numerous program modules have been developed using the computational software Wolfram Mathematica [9, 10]. They implement a wide variety of numerical methods such as the Euler method, Runge-Kutta in their explicit and implicit forms of different orders, as well as the Adams methods in their explicit and implicit forms [11, 12].

Gauss-Legendre methods, which have been used in this paper, are a specific subset of implicit Runge-Kutta methods derived from the collocation of differential equations at Gauss-Legendre quadrature points. This choice makes Gauss-Legendre methods capable of achieving high-order accuracy. The Adams methods included in this paper are chosen so that the number of the previous steps used for computation is identical. This is in order to use the implicit method in combination with the explicit in the predictor-corrector manner [13].

Table 1. Summary of the used methods

Method Name	Notation	Global Error of the Method	Characteristics
Euler	Euler	$\mathcal{O}$(h)	Single step
Runge-Kutta 2nd Order	RK2	$\mathcal{O}$(h²)	Explicit, two intermediate steps
Runge-Kutta 4th Order	RK4	$\mathcal{O}$(h⁴)	Explicit, four intermediate steps
Gauss-Legendre 4th Order	GL4	$\mathcal{O}$(h⁴)	Implicit, increased stability, two steps
Gauss-Legendre 6th Order	GL6	$\mathcal{O}$(h⁶)	Implicit, increased stability, three steps
Explicit Adams 4th Order	EA4	$\mathcal{O}$(h⁴)	Uses 4 previous derivatives
Implicit Adams 4th Order	IA4	$\mathcal{O}$(h⁴)	Uses interpolation for refinement

A summary of the used methods can be seen in Table 1. Implicit numerical methods, renowned for their stability and improved accuracy when dealing with stiff problems, are a focal point in this numerical analysis. The presented work represents an extension of the methods and visualization approaches proposed in [14].

4. Numerical Results

Let us consider the efficiency of various numerical methods with the following parameters: $G = 20, r = 0.1, \alpha = 0.1, \omega = 1, \omega_F = 1, t = 50$. Table 2 shows the expected global theoretical errors T_{err}, the actual error value obtained from the calculations (A_{err}), and the computation time $CT(s)$ for different step sizes h.

The study shows that the best methods are those that apply additional cycles to refine results on a local level (GL4 and GL6). These methods achieve accuracy on the order of 14 decimal places, even with larger step sizes (the step size of the uniform grid used is denoted by h), unlike explicit methods, which work well with smaller step sizes but increase the computation time ($CT(s)$) in seconds.

Table 2. Comparison of the numerical methods with different steps for the parameters $G = 20, r = 0.1, \alpha = 0.1, \omega = 1, \omega_F = 1, t = 50$

Method	h=0.1			h=0.01			h=0.001		
	T_{err}	A_{err}	$CT(s)$	T_{err}	A_{err}	$CT(s)$	T_{err}	A_{err}	$CT(s)$
Euler	10^{-1}	2.9	0.4	10^{-2}	3.5×10^{-1}	0.64	10^{-3}	8.7×10^{-2}	14
RK2	10^{-2}	2.9×10^{-2}	0.1	10^{-4}	2.8×10^{-5}	1.2	10^{-6}	2.8×10^{-8}	19
RK4	10^{-4}	6×10^{-5}	0.2	10^{-8}	1.4×10^{-9}	2	10^{-12}	6.4×10^{-14}	34
GL4	10^{-4}	1.8×10^{-10}	1	10^{-8}	1.7×10^{-15}	11	10^{-12}	6.3×10^{-16}	60
GL6	10^{-6}	1.28×10^{-14}	2	10^{-12}	3.3×10^{-16}	16	10^{-18}	4.4×10^{-15}	119
EA4	10^{-4}	9×10^{-3}	0.1	10^{-8}	2×10^{-7}	2	10^{-12}	1.3×10^{-11}	115
IA4	10^{-4}	4×10^{-4}	0.3	10^{-8}	1.2×10^{-8}	4	10^{-12}	9.2×10^{-13}	167

The comparison of the values of the magnetic moment coordinates found for the set of parameters used in the table can be seen in Fig. 2 through Fig. 7, where the horizontal lines represent the magnetic norm. Also, it can be observed that after an initial imbalance, the system settles into its new state.

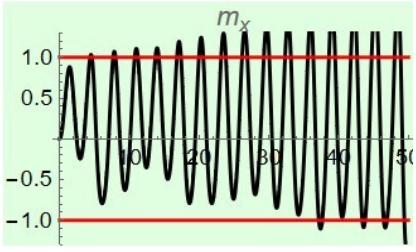


Figure 2. Values of the spatial m_x-coordinate using the Euler method, where h=0.01

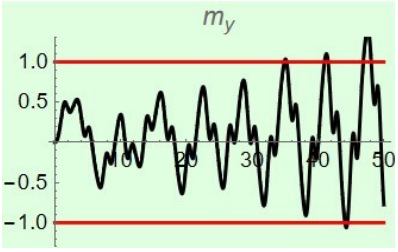


Figure 3. Values of the spatial m_y-coordinate using the Euler method, where h=0.01

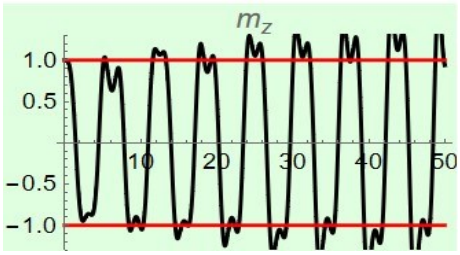


Figure 4. Values of the spatial m_z-coordinate using the Euler method, where h=0.01

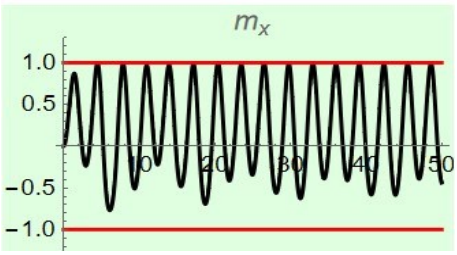


Figure 5. Values of the spatial m_x-coordinate using the Runge-Kutta method, where h=0.01

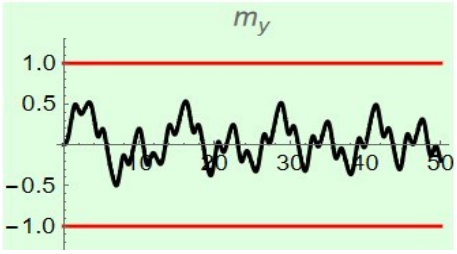


Figure 6. Values of the spatial m_y-coordinate using the Runge-Kutta method, where h=0.01

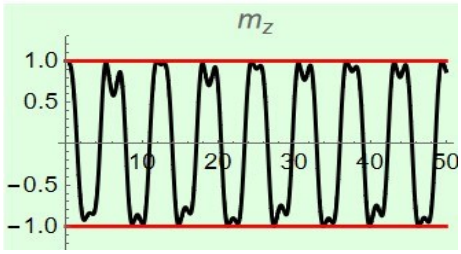


Figure 7. Values of the spatial m_z-coordinate using the Runge-Kutta method, where h=0.01

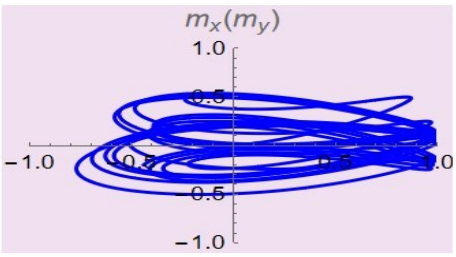


Figure 8. Precession of the magnetic moment in the $m_x(m_y)$ plane

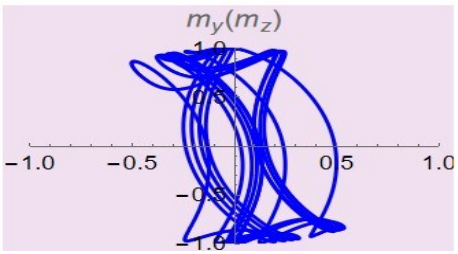


Figure 9. Precession of the magnetic moment in the $m_y(m_z)$ plane

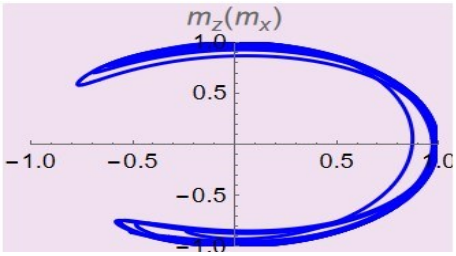


Figure 10. Precession of the magnetic moment in the $m_z(m_x)$ plane

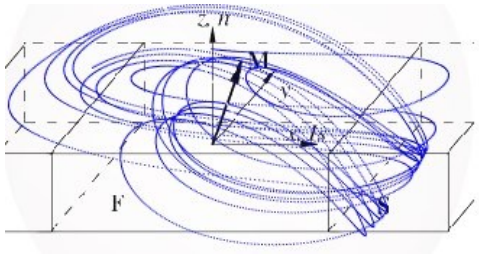


Figure 11. Precession of the magnetic moment in space

The precession of the magnetic moment for the parameters $G = 20, r = 0.1, \alpha = 0.1, \omega = 1, \omega_F = 1, t = 50$ where h=0.01 using the Runge-Kutta method is showcased in Fig. 8 through Fig. 11. Let us examine the numerical results with a different set of parameters. A solution with the following set of parameters $G = 90, r = 0.1,\ \alpha = 0.1, \omega = 0.8,\ \omega_F = 0.8, t = 50$ is presented. After performing the calculations using all methods, we obtain the following results, shown in Table 3.

In this case, it is clear that the chosen set of parameters creates a stiff problem [8,14]. This presents a challenge for numerical methods due to the rapid accumulation of local errors. Trivial methods like the Euler method and EA4 result in the so-called overflow – an inability to continue calculations due to the computer's limitations and computations with excessively large numbers. It can also be seen that even the implicit methods do not meet the expected order of accuracy. However, such cases allow us to assess which methods are more stable when dealing with stiffness. Once again, GL4 and GL6 show the best results in computational accuracy in relation to computational time compared to the other methods used. Also greater accuracy is obtained with a larger step size and relatively less processing capacity. These cases also provide a basis for exploring other, more efficient numerical methods.

In Fig. 12 through Fig. 14 we see that the behaviour of the system seems periodic and shows no signs of settling in the designated period of time. The parameters used are as in Table 3. Also, the rapid changes of the values of the magnetic moment coordinates explain the inability of the trivial methods to cope with the accumulation of local errors. Figure 15. through Fig. 18 show the magnetic moment in the planes and in space.

The precession of the magnetic moment for the parameters $G = 20, r = 0.1, \alpha = 0.1, \omega = 1, \omega_F = 1, t = 50$ where h=0.01 are showcased in Fig. 8 through Fig. 10.

Table 3. Comparison of the numerical methods with different steps for the parameters $G = 90, r = 0.1, \alpha = 0.1, \omega = 0.8, \omega_F = 0.8, t = 50$

Method	h=0.1			h=0.01			h=0.001		
	T_{err}	A_{err}	$CT(s)$	T_{err}	A_{err}	$CT(s)$	T_{err}	A_{err}	$CT(s)$
Euler	10^{-1}	–	–	10^{-2}	6	0.75	10^{-3}	1.4	15
RK2	10^{-2}	7	0.1	10^{-4}	1.7×10^{-2}	1.7	10^{-6}	1.9×10^{-5}	21
RK4	10^{-4}	0.29	0.2	10^{-8}	2.4×10^{-5}	2.3	10^{-12}	1.9×10^{-10}	34
GL4	10^{-4}	3.5×10^{-8}	1.9	10^{-8}	2.6×10^{-12}	10	10^{-12}	3×10^{-11}	88
GL6	10^{-6}	6.7×10^{-12}	3	10^{-12}	1.1×10^{-15}	20	10^{-18}	8.8×10^{-14}	137
EA4	10^{-4}	–	–	10^{-8}	2.7×10^{-4}	2	10^{-12}	2.2×10^{-8}	120
IA4	10^{-4}	2.5×10^{-2}	0.7	10^{-8}	3.3×10^{-5}	7	10^{-12}	3.3×10^{-10}	112

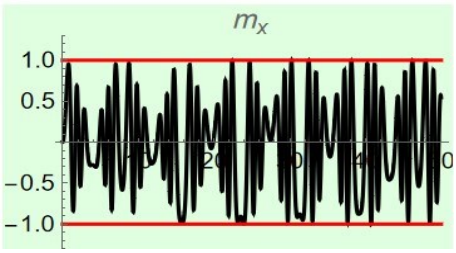


Figure 12. Values of the spatial m_x-coordinate using the Runge-Kutta method, where h=0.01

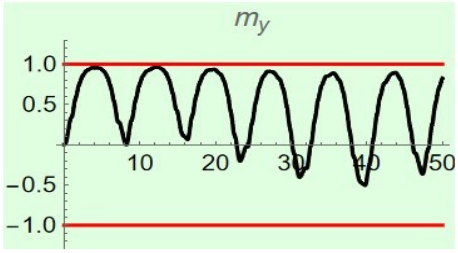


Figure 13. Values of the spatial m_y-coordinate using the Runge-Kutta method, where h=0.01

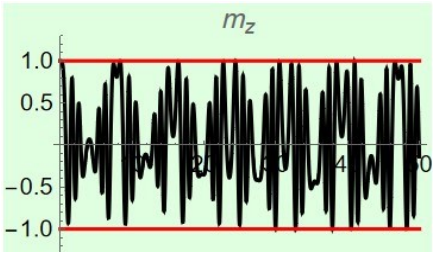


Figure 14. Values of the spatial m_z-coordinate using the Runge-Kutta method, where h=0.01

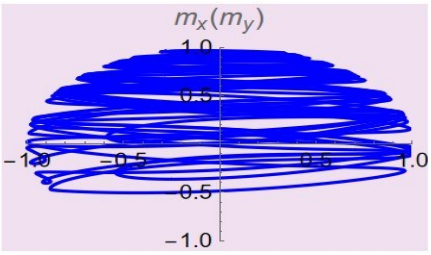


Figure 15. Precession of the magnetic moment in the $m_x(m_y)$ plane

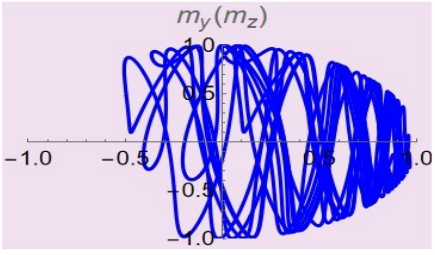


Figure 16. Precession of the magnetic moment in the $m_y(m_z)$ plane

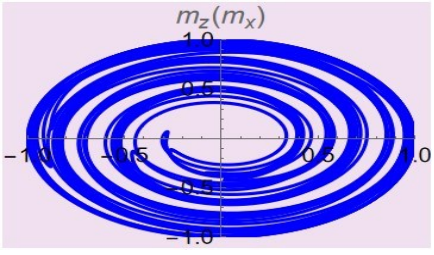


Figure 17. Precession of the magnetic moment in the $m_z(m_x)$ plane

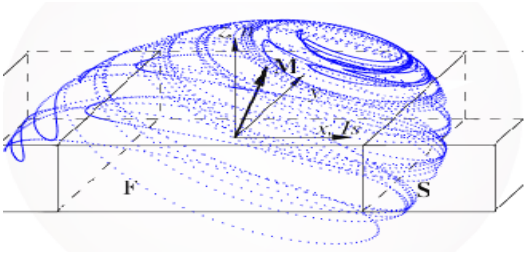


Figure 18. Precession of the magnetic moment in space

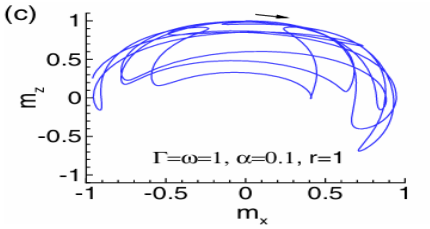


Figure 19. Physical Review Letters 123, 169901(E) (2019)

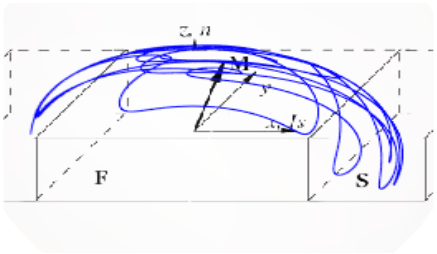


Figure 20. Our results for the identical set of parameters

Verification

This paper has conducted a comparison with other studies and has demonstrated consistent results, further validating the findings. As illustrated in the verification figure provided (Fig. 19 and Fig. 20), the numerical behaviour for the parameters $G = 1, r = 1, \alpha = 0.1, \omega = 1, \omega_F = 1$ observed aligns with those reported in previous research [16].

5. Conclusion

The findings presented in this paper contribute to advancing the understanding of parameter influence on the dynamics of Josephson junction systems. We explored two different sets of parameters to demonstrate the stiffness of the problem under varied conditions. The results underscore the limitations of simpler explicit methods. Conversely, advanced implicit methods achieve high levels of accuracy. By systematically analysing the behaviour of different methods under varying conditions, this research offers valuable insights into the computational challenges associated with modelling complex physical phenomena in Josephson junctions.

Furthermore, this work highlights the importance of numerical strategies in the spintronics field, which plays a critical role in advancing quantum computing. A deeper exploration of these mechanisms is essential for improving the precision and efficiency of models that underlie quantum technologies. Future work may involve refining these methods and exploring more complex junction models with additional physical phenomena.

Future research could involve the implementation of various implicit methods that incorporate adaptive step sizes and stopping criteria to mitigate numerical overflow issues. By optimising the step size dynamically, improvements in computational efficiency and result precision are anticipated. Future investigations may involve magnetic moments with x-coordinate (long JJ) – in such a case we would have to solve a system of partial differential equations [17]. A more general model consider a second harmonic in the current-phase relation - the model includes a double sine-Gordon equation [18].

Acknowledgements

Special thanks are extended to Pavlina Atanasova and Stanka Hadzhikoleva for their support, valuable advice, constructive criticism, and insightful comments.

References

[1] Borzì, A. (2020). *Modelling with ordinary differential equations: a comprehensive approach*. Chapman and Hall/CRC. https://doi.org/10.1201/9781351190398

[2] Bobkov, G. A., Bobkova, I. V., & Bobkov, A. M. (2024). Controllable magnetic states in chains of coupled φ0-Josephson junctions with ferromagnetic weak links. *Physical Review B*, *109*(5), 054523. https://doi.org/10.1103/PhysRevB.109.054523

[3] Nashaat, M., Kovalenko, E., & Shukrinov, Y. M. (2024). Buzdin, Shapiro, and chimera steps in φ0-Josephson junctions. II. Bifurcation, switching, and hysteresis. *Physical Review B*, *110*(2), 024510. https://doi.org/10.1103/PhysRevB.110.024510

[4] Buzdin, A. (2008). Direct coupling between magnetism and superconducting current in the Josephson φ0-junction. *Physical review letters*, *101*(10), 107005. https://doi.org/10.1103/PhysRevLett.101.107005

[5] Atanasova, P. K. H., Boyadjiev, T. L., Shukrinov, Y. U. M., Zemlyanaya, E. V., & Seidel, P. (2010). Influence of Josephson current second harmonic on stability of magnetic flux in long junctions. In Journal of Physics: Conference Series (Vol. 248, No. 1, p. 012044). IOP Publishing. https://doi.org/10.1088/1742-6596/248/1/012044

[6] Atanasova, P. K., Zemlyanaya, E. V., & Shukrinov, Y. M. (2012). Interconnection between static regimes in the LJJs described by the double sine-Gordon equation. In *Journal of Physics: Conference Series* (Vol. 393, No. 1, p. 012023). IOP Publishing. https://doi.org/10.1088/1742-6596/393/1/012023

[7] Shukrinov, Y. M., Rahmonov, I. R., Sengupta, K., & Buzdin, A. (2017). Magnetization reversal by

superconducting current in φ Josephson junctions. *Applied Physics Letters*, *110*(18). https://doi.org/10.1063/1.4983090

[8] Atanasova, P. K., Panayotova, S. A., Zemlyanaya, E. V., Shukrinov, Y. M., & Rahmonov, I. R. (2019). Numerical simulation of the stiff system of equations within the spintronic model. In *Numerical Methods and Applications: 9th International Conference, NMA 2018, Borovets, Bulgaria, August 20-24, 2018, Revised Selected Papers 9* (pp. 301-308). Springer International Publishing. https://doi.org/10.1007/978-3-030-10692-8_33

[9] Atanasova, P., Panayotova, S., Shukrinov, Y., Rahmonov, I., & Zemlyanaya, E. (2018). User Software for Numerical Study of Josephson Junction with Magnetic Momenta. In *EPJ Web of Conferences* (Vol. 173, p. 05002). EDP Sciences. https://doi.org/10.1051/epjconf/201817305002

[10] Wolfram, "Official website of Wolfram Mathematica," Wolfram, Jul. 5, 2024. [Online]. Available: https://www.wolfram.com/mathematica/.

[11] Boyanov, B. & Semerdzhiev, H. (1988) Numerical Methods, Publ. Paisii Hilendarski University of Plovdiv.

[12] Butcher, J. C. (1964). Implicit runge-kutta processes. *Mathematics of computation*, *18*(85), 50-64. https://doi.org/10.2307/2003405

[13] Hairer, E., Nørsett, S. P. & Wanner, G. (1987) *Solving Ordinary Differential Equations I*. Springer-Verlag. https://doi.org/10.1007/978-3-662-12607-3

[14] Atanasova, P. K., Panayotova, S. A., Zemlyanaya, E. V., Shukrinov, Y. M., & Rahmonov, I. R. (2019). Numerical simulation of the stiff system of equations within the spintronic model. In *Numerical Methods and Applications: 9th International Conference, NMA 2018, Borovets, Bulgaria, August 20-24, 2018, Revised Selected Papers 9* (pp. 301-308). Springer International Publishing. https://doi.org/10.1007/978-3-030-10692-8_33

[15] Hall, G. G., & Watt, J. M. (1976). *Modern numerical methods for ordinary differential equations*. Oxford, U.K.: Clarendon Press.

[16] Konschelle, F., & Buzdin, A. (2009). Magnetic moment manipulation by a Josephson current. *Physical Review Letters*, *102*(1), 017001. https://doi.org/10.1103/PhysRevLett.102.017001

[17] Atanasova, P. K., Boyadjiev, T. L., Shukrinov, Y. M., & Zemlyanaya, E. V. (2011). Numerical modeling of long Josephson junctions in the frame of double sine-Gordon equation. *Mathematical Models and Computer Simulations*, *3*, 389-398. https://doi.org/10.1134/S2070048211030033

[18] Atanasova, P. & Georgiev, V. (2023) Numerical solving of the sine-Gordon equation. In *Proceedings of the International Scientific Conference "Informatics, Mathematics, Education and Their Applications"* (IMEA 2023), Pamporovo, Bulgaria, Nov. 29–Dec. 1, 2023, Plovdiv University Press, pp. 23–30, ISBN: 978-619-7663-79-2.